JOURNAL OF VIROLOGY, Mar. 2005, p. 3595–3605 Vol. 79, No. 6
0022-538X/05/$08.00+0 doi:10.1128/JVI.79.6.3595–3605.2005
Copyright © 2005, American Society for Microbiology. All Rights Reserved.

# The Influenza A Virus $M_2$ Cytoplasmic Tail Is Required for Infectious Virus Production and Efficient Genome Packaging

Matthew F. McCown[1] and Andrew Pekosz[1,2]*

*Departments of Molecular Microbiology[1] and Pathology and Immunology,[2] Washington University School of Medicine, St. Louis, Missouri*

Received 24 June 2004/Accepted 21 October 2004

**The $M_2$ integral membrane protein encoded by influenza A virus possesses an ion channel activity that is required for efficient virus entry into host cells. The role of the $M_2$ protein cytoplasmic tail in virus replication was examined by generating influenza A viruses encoding $M_2$ proteins with truncated C termini. Deletion of 28 amino acids ($M_2$Stop70) resulted in a virus that produced fourfold-fewer particles but >1,000-fold-fewer infectious particles than wild-type virus. Expression of the full-length $M_2$ protein in *trans* restored the replication of the $M_2$ truncated virus. Although the $M_2$Stop70 virus particles were similar to wild-type virus in morphology, the $M_2$Stop70 virions contained reduced amounts of viral nucleoprotein and genomic RNA, indicating a defect in vRNP packaging. The data presented indicate the $M_2$ cytoplasmic tail plays a role in infectious virus production by coordinating the efficient packaging of genome segments into influenza virus particles.**

Influenza A virus particles contain eight RNA strands that are organized into viral nucleoprotein complexes (vRNPs) by association with several viral proteins. Packaging of vRNPs into virus particles is thought to occur at glycolipid rafts at the plasma membrane and may be mediated by interactions between the vRNPs, the viral matrix protein ($M_1$), and the cytoplasmic tails of the integral membrane proteins hemagglutinin (HA) and neuraminidase (NA) (68). The precise interactions that mediate infectious virus particle production are not understood in great detail. It is clear the viral $M_1$ protein can mediate budding when expressed alone or in concert with other viral proteins (13, 14, 32, 41). The viral RNA segments contain unique packaging signals that overlap the open reading frames in certain RNA segments, implying coordinated packaging of influenza virus genomic segments exists (12, 62). The cytoplasmic tails of the HA and NA integral membrane proteins appear to be essential to maintain virion morphology and association of HA and NA with glycolipid rafts is required for efficient virus production (3, 28, 54, 68).

The $M_2$ protein of influenza A virus is translated from a spliced mRNA derived from RNA segment seven and is present in the plasma membrane of virus-infected or cDNA transfected cells as a disulfide-linked tetramer (21, 30, 31, 67). The requirement for $M_2$ ion channel activity during influenza A virus entry into cells has been well documented (4, 5, 19, 34, 49, 53). Briefly, influenza A virus binds to sialic acid residues on the plasma membrane and is internalized via clathrin-dependent and -independent mechanisms (29). Acidification of virus-containing endosomes activates the $M_2$ ion channel activity, inducing the translocation of $H^+$ ions into the virion interior (9, 49). This flux of $H^+$ ions is predicted to disrupt interactions between the vRNPs, $M_1$, and the viral membranes, allowing the vRNPs to diffuse away from the endosomal membrane and toward the cell nucleus once virus-cell membrane fusion is completed (35, 69, 70). The antiviral drugs rimantadine and amantadine bind to the transmembrane domain of the $M_2$ tetramer, thereby inhibiting proton translocation (58).

Evidence for an effect of $M_2$ on influenza A virus assembly comes from studies of anti-$M_2$ antibody-mediated inhibition of influenza virus replication (65). Antibodies that recognize the extracellular domain of $M_2$ are capable of reducing virus budding and preventing the formation of filamentous influenza A virus particles (24, 51). Escape variants that are no longer sensitive to anti-$M_2$ antibodies contain mutations in the $M_2$ cytoplasmic tail, as well as the $M_1$ protein (64). The effect of anti-$M_2$ antibodies on virus assembly is all the more surprising when one considers the low amount of $M_2$ that is incorporated into virions (65).

Reverse genetics studies on the role of $M_2$ in virus replication have given conflicting results with respect to the requirement of an $M_2$ ion channel activity for efficient virus replication in vitro (55, 61). This is not completely surprising, given the fact that different virus strains were used and amantadine has a strain-dependent effect on influenza A virus replication (19). It is clear, however, that deletion of the $M_2$ transmembrane and cytoplasmic tail regions result in a virus that is highly attenuated for in vitro replication—much more so than viruses that encode $M_2$ proteins with defects in ion channel activity alone (61). Reduced expression of $M_2$ by $M_2$-specific small interfering RNAs resulted in a decrease in total, as well as infectious, virion production, providing further evidence that $M_2$ may be involved in virus assembly (36).

These and other results suggested to us that a detailed investigation of the $M_2$ cytoplasmic tail and its role in virus replication was needed. A series of deletions in the $M_2$ cytoplasmic tail were introduced into recombinant viruses by using a reverse genetics approach. We show that a 28-amino-acid deletion of the $M_2$ cytoplasmic tail resulted in a fourfold de-

* Corresponding author. Mailing address: Department of Molecular Microbiology, Washington University School of Medicine, Campus Box 8230, 660 S. Euclid Ave., St. Louis, MO 63110-1093. Phone: (314) 747-2132. Fax: (314) 362-3203. E-mail: pekosz@borcim.wustl.edu.

crease in particle formation but a 1,000-fold decrease in virus infectivity. The truncated $M_2$ protein retained its ion channel activity and could be incorporated into virions, implying the cytoplasmic tail deletion was responsible for the attenuation. The virus encoding a truncated $M_2$ protein was found to incorporate reduced amounts of NP and genomic RNA. Complementation with full-length $M_2$ restored infectivity, as well as nucleoprotein (NP) and genomic RNA incorporation, suggesting the $M_2$ cytoplasmic tail is important for genome packaging and infectious virus production.

## MATERIALS AND METHODS

**Plasmids.** The plasmid pCAGGS (pC) (42) encoding the cDNA for the full-length $M_2$ protein from A/Udorn/72 (pC $M_2$) has been described previously (36) and was used to express the $M_2$ protein. By using PCR mutagenesis, the pCAGGS $M_2$ vector was altered so that a stop codon was introduced at amino acid 90 (pC $M_2$Stop90), at amino acid 82 (pC $M_2$Stop82), and at amino acid 70 (pC $M_2$Stop70). The cDNA for the HA gene from A/chicken/Germany/34 (FPV Rostock), courtesy Robert Lamb, was cloned between the SacI and XhoI sites of the pCAGGS vector (pC FPV HA). The plasmid pBABE, which expresses puromycin *N*-acetyltransferase under control of the simian virus 40 promoter, was used to generate stable cell transformants resistant to puromycin. The plasmids pRevTet-On and pREV-TRE were purchased from Clontech. The cDNA for $M_2$ from A/Udorn/72 was blunt end cloned into the Klenow-filled SalI site of pREV-TRE.

In order to generate a standard curve for real-time reverse transcription-PCR (RT-PCR) assays, the $M_1$ (A/Udorn/72) open reading frame (nucleotides 26 to 784) was cloned into the KpnI and SphI cloning sites of pGEM-3 (Promega) creating pGEM-3-$M_1$. A runoff transcription reaction was performed utilizing the MEGAscript SP6 kit (Ambion) and PshAI-digested pGEM-3-$M_1$ resulting in a 761-nucleotide transcript. The RNA was quantified by spectrometry, divided into aliquots, and stored at −70°C.

To generate recombinant viruses that contain truncations in the $M_2$ protein, the plasmid pHH21 M-Udorn, encoding the A/Udorn/72 M segment under control of the human RNA polymerase I promoter and murine RNA polymerase I terminator (55), was altered by using PCR mutagenesis. The plasmid pHH21 M-Ud $M_2$Stop90 has two in-frame stop codons introduced in place of amino acids 90 and 91, pHH21 M-Ud $M_2$Stop82 has two in-frame stop codons introduced in place of amino acids 82 and 83, and pHH21 M-Ud $M_2$Stop70 has two in-frame stop codons introduced in place of amino acids 70 and 71.

All plasmids were purified from overnight bacterial cultures by using the Qiagen MaxiPrep kit and resuspended in water. All primer sequences are available upon request.

**Cells.** Madin-Darby canine kidney cells (MDCK) and human embryonal kidney cells (293T) were cultured in Dulbecco modified Eagle medium (DMEM) containing 10% fetal bovine serum, 100 U of penicillin/ml, and 100 μg of streptomycin/ml. The HB-64 and HB-65 hybridomas were cultured in DMEM containing 10% fetal bovine serum, 100 U of penicillin/ml, and 100 μg of streptomycin/ml. For antibody collection, the cells were grown to confluence and the serum-containing media was replaced with RPMI 1640 media containing10% hybridoma enhancing supplement (Sigma), 100 U of penicillin/ml, and 100 μg of streptomycin/ml. The cells were cultured for 5 to 7 days before cell-free supernatants were collected.

**Antibodies.** The anti-$M_2$ monoclonal antibody (MAb) 14C2 recognizes an epitope in the extracellular domain of $M_2$ (65). The HB-65 MAb recognizes the NP and the HB-64 MAb recognizes the $M_1$ protein (63). The antibody that recognizes HA is a polyclonal goat anti-H0 A/PR/8/34 (V-314-511-157; National Institute of Allergy and Infectious Diseases). Species-specific immunoglobulin G (IgG) secondary antibodies used in the present study were purchased from Jackson Laboratories. A rabbit polyclonal sera recognizing the FPV HA protein was provided by Robert Lamb and used for FPV HA immunoprecipitations.

**Stable and inducible cell lines.** Stable MDCK cell lines expressing $M_2$ or $M_2$Stop70 were established by cotransfecting the plasmid pBABE with pC $M_2$ or pC $M_2$Stop70 by using Lipofectamine 2000 (Invitrogen, Carlsbad, Calif.) according to the manufacturer's protocol. At 24 h posttransfection the cells were detached with trypsin, plated at a 1:5 density, and cultured in medium containing 7.5 μg of puromycin/ml and 5 μM amantadine hydrochloride (Sigma). The puromycin-resistant cell population was enriched by fluorescence-activated cell sorting (FACS) as described below.

To generate MDCK cells that are capable of expressing $M_2$ protein upon tetracycline treatment, the vectors pRevTet-On and pRevTRE-$M_2$ (Clontech) were used. Retroviruses were generated by using pRevTet-On according to the manufacturer's protocol and used to transduce MDCK cells. The transduced cells were selected with 1.3 mg of Geneticin/ml (Gibco-BRL), and the resulting cell population (MDCK-Tet-On) was transfected with pRevTRE-$M_2$ by using Lipofectamine 2000. At 24 h posttransfection the cells were selected with 1.3 mg of Geneticin/ml and 0.4 mg of hygromycin/ml. At 24 h after induction of $M_2$ expression by the addition of 1 μg of doxycycline/ml to the culture medium, the $M_2$-expressing cells were enriched for by FACS as described below.

**FACS.** The cells were detached and stained by using the anti-$M_2$ MAb 14C2 (1:1,000 dilution) or anti-$M_1$ MAb HB64 hybridoma supernatant (1:50 dilution), followed by goat anti-mouse IgG (fluorescein isothiocyanate labeled; Jackson Laboratories) secondary antibody. For $M_1$ staining, cells were permeabilized by including 0.1% saponin in all antibody dilutions and wash buffers (47). The cells were analyzed by flow cytometry (FACSCalibur dual laser flow cytometer; Becton Dickinson) by using CellQuest software. When required, the cells positive for $M_2$ expression were gated, sorted, and expanded.

**Viruses.** The recombinant influenza A viruses used in the present study are rWSN M-Udorn, rWSN M-Udorn $M_2$Stop90 (codons 90 and 91 mutated to stop codons), and rWSN M-Udorn $M_2$Stop70 (codons 70 and 71 mutated to stop codons). rWSN M-Ud contains seven segments derived from A/WNS/33 and an M segment derived from A/Udorn/72 (55, 61). rWSN M-Ud $M_2$Stop90 was generated by using the 12 plasmid rescue system in 293T cells (40). Briefly, 293T cells are transfected with plasmids encoding the eight influenza A virus genomic segments as well as plasmids expressing the PA, PB1, PB2, and NP proteins, which make up the functional influenza A virus polymerase complex (23). rWSN M-Ud $M_2$Stop70 was generated by transfecting 293T cells and coculturing the cells with MDCK-$M_2$ cells, according to the protocol used by Takeda et al. for the recovery of recombinant influenza A/Udorn/72 virus (55). The resulting viruses were confirmed by sequencing the M segment.

Influenza A virus particles were quantitated by hemagglutination of 0.5% chicken red blood cells (44). The infectious virus titer was determined by plaque assay on MDCK or MDCK-$M_2$ cells (44), and the viral M segment of all viruses was sequenced to ensure that no unwanted mutations were present.

**Virus infections.** Virus stocks and low multiplicity of infection (MOI) growth curves were generated by infecting cells at an MOI of 0.01; incubating the cells at 37°C in DMEM containing 1 μg of acetyl trypsin (Sigma Chemicals), penicillin, and streptomycin/ml; and harvesting infected cell supernatants at the indicated times (72 h postinfection for viral stocks). Virus stocks of rWSN M-Ud $M_2$Stop70 were generated by infection of MDCK-$M_2$ cells.

Virions were analyzed by infecting cells with rWSN M-Ud or rWSN M-Ud $M_2$Stop70 at an MOI of 1.0. The cells were infected for 1 h at room temperature, washed extensively with phosphate-buffered saline (PBS), and incubated in DMEM containing penicillin and streptomycin for 15 h at 37°C. The medium was harvested, and cell debris was removed by a low-speed centrifugation. The cleared supernatant was layered onto a 10% sucrose cushion in PBS and centrifuged at 178,000 × *g* (38,000 rpm in an SW41 rotor) for 1 h. The supernatant was removed, and the pellet was resuspended in PBS.

**$TCID_{50}$ assay.** MDCK-Tet$M_2$ cells were plated in a 96-well plate and left untreated or treated with 1 μg of doxycycline/ml for 24 h. After induction, the cells were infected with serial dilutions, in triplicate, of rWSN M-Ud or rWSN M-Ud $M_2$Stop70 in DMEM containing 1 μg of acetyl trypsin, penicillin, and streptomycin/ml and 1 μg of doxycycline/ml for the samples previously induced. The infection proceeded for 72 h at 37°C, the cells were stained with naphthol blue black, and the cytopathic effect was scored visually. A Reed and Muench calculation was used to determine the 50% tissue culture infective dose ($TCID_{50}$) (50).

**Metabolic labeling.** 293T cells were transfected with the indicated plasmids by using LT1 (Mirus Corp., Madison, Wis.) or infected at an MOI of 1.0. At 24 h posttransfection or 12 h postinfection, the cells were incubated for 30 min in DMEM without methionine or cysteine (DMEM-Met/$Cys^-$). The cells were then incubated for 15 min in DMEM-Met/$Cys^-$ containing 2 mM methionine and 50 μCi of [$^{35}$S]cysteine (Amersham Biosciences). The cells were incubated for the indicated times in chase media (DMEM containing 10% fetal bovine serum, penicillin, and streptomycin) and lysed in 1% TX-100, 50 mM NaCl, 10 mM Tris (pH 7.5), 5 mM EDTA, 5 mM iodoacetamide, and a protease inhibitor cocktail. The lysate was clarified by centrifugation at 14,000 × *g* in a microcentrifuge at 4°C.

**FPV HA rescue assay.** $M_2$ ion channel activity was determined by transfecting 293T cells with pC FPV HA and either pC, pC $M_2$, or pC $M_2$Stop70. The samples were transfected in duplicate, and one sample was incubated with 5 μM amantadine 6-h posttransfection. At 24 h posttransfection the cells were incubated for 30 min in DMEM-Met/$Cys^-$ containing 25 mM HEPES (pH 6.8) and 5 μM

TABLE 1. Sequence of the predicted cytoplasmic tail for $M_2$ and truncation mutants

| Protein | Sequence[a] at position: | | | | | |
|---|---|---|---|---|---|---|
| | 44 | 54 | 64 | 74 | 84 | 94 |
| $M_2$ | DRLFFKCIYR | FFEHGLKRGP | STEGVPESMR | EEYRKEQQSA | VDADDSHFVS | IELE |
| $M_2$Stop90 | DRLFFKCIYR | FFEHGLKRGP | STEGVPESMR | EEYRKEQQSA | VDADDS** | |
| $M_2$Stop82 | DRLFFKCIYR | FFEHGLKRGP | STEGVPESMR | EEYRKEQQ** | | |
| $M_2$Stop70 | DRLFFKCIYR | FFEHGLKRGP | STEGVP** | | | |
| $M_2$Stop 70 Revertant[b] | DRLFFKCIYR | FFEHGLKRGP | STEGVP**WW**MR | VEYRKEQQSA | VDADDSHFV**G** | **V**ELE |

[a] **, Two in-frame stop codons. Bold letters indicate amino acids changes in the revertant virus. The underlined letter indicates an amino acid changed in the plasmid used to generate the $M_2$Stop 70 virus.
[b] In addition to the mutations indicated in $M_2$, there was an additional Ala-to-Thr change in $M_1$ at position 22.

amantadine (for treated samples). The cells were then incubated for 15 min in DMEM-Met/Cys$^-$ containing 25 mM HEPES (pH 6.8), 5 μM amantadine (for treated samples), and 100 μCi of Pro-Mix $^{35}$S in vitro cell labeling mix (Amersham) (56). The cells were incubated for the indicated times in chase medium containing 25 mM HEPES (pH 6.8) and lysed in 1% NP-40, 50 mM Tris (pH 7.5), 5 mM EDTA, and protease inhibitors. The lysate was clarified by centrifugation at 14,000 × *g* in a microcentrifuge at 4°C.

**Immunoprecipitations.** Clarified supernatants were incubated with MAb 14C2 (1:100 dilution) or anti-FPV sera (1:300) at 4°C for 2 h. Protein G Plus/Protein A Agarose (Oncogene), diluted with Sepharose CL-4B (Sigma) in a 1:2 mixture, was added for 30 min. The Protein G Plus/Protein A agarose was pelleted, washed with radioimmunoprecipitation assay buffer (1% sodium deoxycholate, 1% Triton X-100, 0.1% sodium dodecyl sulfate [SDS], 10 mM Tris [pH 7.5], 0.5 M NaCl) four times and once in SDS wash II (150 mM NaCl, 50 mM Tris [pH 7.5], 2.5 mM EDTA). The beads were then resuspended in 2× SDS-PAGE sample buffer.

**SDS-PAGE and Western blotting.** Infected cells were lysed in 1% SDS and mixed at a 1:1 ratio with 2× SDS-PAGE sample buffer. Purified virions were resuspended in 2× SDS-PAGE sample buffer. Samples were loaded onto either a 15% polyacrylamide gel or a 17.5% polyacrylamide gel with 4 M urea.

For immunoprecipitation experiments, the gel was soaked in a fixative solution (8.5% acetic acid, 20% methanol) two times for 10 min each, followed by a 10-min wash in 1% glycerol in $H_2O$. The gel was dried on a gel dryer (Model 583 Gel Dryer; Bio-Rad), imaged by exposure to a phosphorimager plate (Fuji Medical Systems), and read by a phosphorimager (FujiFilm FLA-5000).

For Western blotting, the separated polypeptides were transferred onto polyvinylidene difluoride membranes (Mini Trans-Blot; Bio-Rad) and blocked in PBS containing 0.3% Tween 20 and 5% dry milk. Primary antibodies were detected by using species-specific IgG secondary antibodies coupled to horseradish peroxidase (Jackson Laboratories). The blots were imaged (Amersham Biosciences ECL Plus) by using either chemiluminescence and exposure to X-ray film (Molecular Technologies) or chemifluorescence and instrument scanning (FujiFilm FLA-5000) to determine the band intensity.

In order to determine polypeptide composition of the virions, equal volumes of pelleted virions were loaded onto SDS–15% polyacrylamide gel electrophoresis (PAGE) gels and the polypeptides separated. Western blotting and quantitation against HA0 (antibody dilution 1:500) was performed. Additional gels were then loaded so that equal amounts of HA protein were loaded for each sample. The incorporation of the influenza A virus $M_1$ (antibody dilution 1:200) and NP (antibody dilution 1:50) proteins were then examined by Western blot.

**Negative stain electron microscopy.** Purified virions were allowed to absorb onto Formvar/carbon-coated nickel grids for 5 min. Grids were then washed in $dH_2O$ and stained with 1% aqueous uranyl acetate (Ted Pella, Inc., Redding, Calif.) for 1 min. Excess liquid was gently wicked off, and grids were allowed to air dry. Samples were viewed on a JEOL 1200EX transmission electron microscope (JEOL USA, Peabody, Mass.).

**Semiquantitative RT-PCR and real-time RT-PCR.** RNA was extracted from infected-cell supernatants by using the QIAamp Viral RNA Minikit (Qiagen) according to the manufacturer's instructions. RNA was extracted from purified virions by the addition of proteinase K (final concentration, 0.5 μg/ml) and SDS (final concentration, 0.5%), followed by incubation for 15 min at 37°C (46). Low pH phenol and low pH phenol: chloroform extractions were performed and the RNA was precipitated by the addition of 1/10 volume of 3.0 M sodium acetate pH 5.4 and 2.5 volumes of ethanol, followed by incubation at −20°C for 20 min and centrifugation at 15,000 × *g* for 15 min in a microcentrifuge. The RNA pellets were washed with 70% ice-cold ethanol, dried, and resuspended in RNase-free water. For the semiquantitative RT-PCR and real-time RT-PCR, an HA assay was performed prior to RNA extraction so that an equivalent number of virions would be analyzed. Primers specific for the influenza A virus NS, M, or NP segment were used for the semiquantitative RT-PCR. Starting at cycle 10 and then after every five cycles, aliquots were removed from each sample. The aliquots were loaded on a 1% agarose gel, separated, and visualized with ethidium bromide fluorescence. The real-time RT-PCR assay was performed essentially as described previously (59), utilizing the TaqMan EZ RT-PCR core reagents (Applied Biosystems) and an ABI 7000 Sequence Detection System (Applied Biosystems). A standard curve was generated by using serial dilutions of an in vitro transcribed, M segment-derived RNA transcript.

## RESULTS

**Stability and surface expression of $M_2$ proteins with truncations in the cytoplasmic tail.** The cDNA encoding $M_2$, from A/Udorn/72, was altered such that stop codons were introduced in place of amino acid 90 (pC $M_2$Stop90), amino acid 82 (pc $M_2$Stop82), and amino acid 70 (pc $M_2$Stop70). The amino acid sequence of the cytoplasmic tail of $M_2$ and the truncated proteins is shown in Table 1. 293T cells were transfected with plasmids encoding the wild-type or truncated proteins, metabolically labeled with [$^{35}$S]cysteine, and chased for 0 to 180 min, and the cell lysates were immunoprecipitated with the MAb 14C2. After a 180-min chase, 97% of the full-length $M_2$ protein still remained (Fig. 1A). All three of the truncation mutants were slightly less stable than the full-length protein, with ca. 70% remaining after 180 min.

The steady-state cell surface expression of the truncated $M_2$ proteins was determined by transfecting 293T cells with plasmids encoding the wild-type or truncated proteins and measuring cell surface expression by flow cytometry. There was no significant difference in either the number of cells expressing the truncated $M_2$ proteins or the amount of protein expressed (as determined by the mean channel fluorescence) compared to the full-length $M_2$ protein (Table 2).

**Ion channel activity of $M_2$ proteins with cytoplasmic tail truncations.** As a surrogate for electrophysiological assays that measure ion channel activity directly in mammalian cells (6, 37–39), the ability of the $M_2$Stop70 protein to alter intracellular transport and proteolytic cleavage of the FPV HA protein was measured. This assay has been utilized to measure the proton channel activity of $M_2$ (7, 8, 43, 52, 56), as well as other viral proton channels (16, 39). The FPV HA protein is cleaved from its full-length (HA0) into a disulfide-linked dimer (HA1 and HA2) by furin-like enzymes in the *trans*-Golgi in the absence of $M_2$ (Fig. 1B). In the presence of $M_2$ a majority of the protein remains as HA0, a result of pH perturbations in the

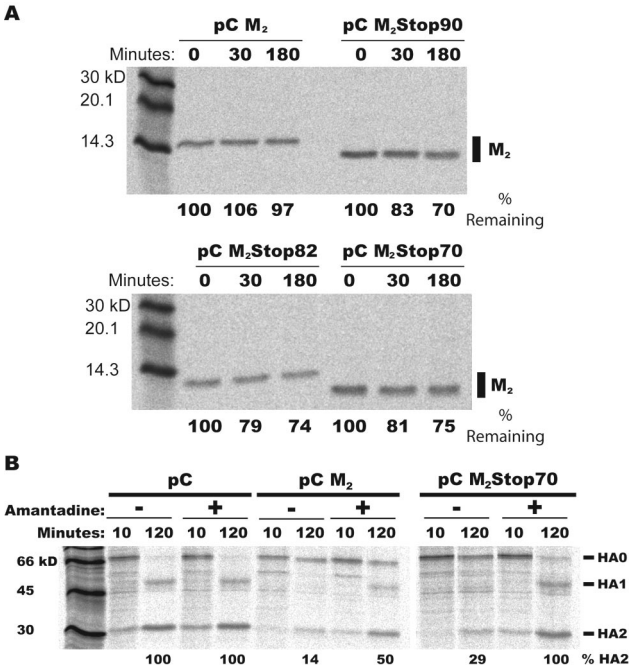


FIG. 1. Effect of $M_2$ cytoplasmic tail truncations on protein stability and ion channel activity. (A) 293T cells expressing the indicated $M_2$ protein were metabolically labeled, and cell lysates were immunoprecipitated with an MAb to $M_2$. The proteins were separated by SDS-PAGE and visualized by using a phosphorimager. (B) 293T cells transfected with pC FPV HA and pC, pC $M_2$, or pC $M_2$Stop70 were metabolically labeled, cell lysates were generated at the indicated times, and immunoprecipitations were performed with polyclonal sera against FPV HA. The proteins were separated by SDS-PAGE and visualized with a phosphorimager. The amount of labeled HA2, for each sample, after a 120-min chase was normalized to the pC sample without amantadine.

Golgi cisternae (8, 15) mediated by the ion channel activity of $M_2$ (16, 39), resulting in reduced intracellular transport rates for integral membrane proteins (20, 52). The reduced processing and intracellular transport of FPV HA can be relieved by the addition of amantadine, demonstrating that retention is a result of $M_2$ ion channel activity and not simply overexpression of $M_2$ protein. Similar results were achieved when $M_2$Stop70 was used in place of full-length $M_2$, indicating the cytoplasmic tail truncation does not drastically alter the ion channel activity (Fig. 1B).

TABLE 2. Cell surface expression of $M_2$ and truncation mutants from cDNA and virus expression

| Expression vector[a] | Infected cell[b] | $M_2$ | | $M_1$ | |
|---|---|---|---|---|---|
| | | % Cells positive | Mean channel fluorescence | % Cells positive | Mean channel fluorescence |
| pC $M_2$ | | 39 | 468 | | |
| pC $M_2$Stop90 | | 32 | 463 | | |
| pC $M_2$Stop82 | | 35 | 452 | | |
| pC $M_2$Stop70 | | 38 | 412 | | |
| | rWSN M-Ud | 87 | 298 | 96 | 168 |
| | rWSN M-Ud $M_2$Stop90 | 26 | 66 | 96 | 191 |
| | rWSN M-Ud $M_2$Stop70 | 3 | 52 | 92 | 176 |

[a] 293T cells were used in the transfection experiments.
[b] MDCK cells were used in the infection experiments.

**Generation of influenza A viruses with truncations in the cytoplasmic tail of $M_2$.** Using the influenza A virus 12-plasmid reverse genetics system (40), we were successful in rescuing a virus that encoded the $M_2$ protein with the smallest truncation (rWSN M-Ud $M_2$Stop90). The influenza A virus rescue system was altered so that 293T cells were cocultured with MDCK-$M_2$ cells, a stable cell line with ca. 50% (mean channel fluorescence of 337) of the population expressing the full-length $M_2$ protein (Fig. 2A). Using this coculture method, the virus that encodes the largest truncation (rWSN M-Ud $M_2$Stop70) was successfully rescued. It is not obvious why we were unsuccessful at rescuing rWSN M-Ud $M_2$Stop82; one possibility is that the ion channel activity of this protein is altered, whereas smaller and larger truncations do not affect the ion channel activity of $M_2$ (57).

**Replication of influenza A viruses encoding for truncations in the cytoplasmic tail of $M_2$.** Fig. 2B examines the ability of rWSN M-Ud $M_2$Stop70 to form plaques either on MDCK or MDCK-$M_2$ cells. The rWSN M-Ud $M_2$Stop70 virus was unable to form discernible plaques on MDCK cells, but plaques were clearly evident when the same inoculum was used to infect MDCK-$M_2$ cells, indicating the expression of full-length $M_2$ protein in *trans* is sufficient to restore rWSN M-Ud $M_2$Stop70 virus plaque formation.

A multiple-step growth curve was performed on MDCK and MDCK-$M_2$ cells with rWSN M-Ud, rWSN M-Ud $M_2$Stop90, or rWSN M-Ud $M_2$Stop70 (Fig. 2C). rWSN M-Ud and rWSN M-Ud $M_2$Stop90 replicated with similar kinetics and produced a similar amount of infectious virus when either MDCK or MDCK-$M_2$ cells were infected. In contrast, rWSN M-Ud $M_2$Stop70 replicated with similar kinetics and produced a similar amount of infectious virus only in the MDCK-$M_2$ cells; infection of wild-type MDCK cells resulted in an ~1,000-fold-lower level of infectious virus production. These data demonstrates that full-length $M_2$ protein expression in *trans* can restore efficient virus replication to the rWSN M-Ud $M_2$Stop70 virus.

**Stability and expression of $M_2$ proteins with truncations in the cytoplasmic tail expressed during virus infection.** 293T cells were infected with rWSN M-Ud, rWSN M-Ud $M_2$Stop90, or rWSN M-Ud $M_2$Stop70. At 12 h postinfection the cells were metabolically labeled with [$^{35}$S]cysteine, and the cell lysates were immunoprecipitated with 14C2. The $M_2$ proteins expressed in rWSN M-Ud- and rWSN M-Ud $M_2$Stop90-infected cells displayed similar stabilities (Fig. 3A), a finding consistent with their stability when expressed from cDNA (see Fig. 1A). However, the amount of $M_2$Stop70 protein expressed during rWSN M-Ud $M_2$Stop70 infection was significantly reduced at both 0 and 180 min compared to the amount of wild-type $M_2$ or $M_2$Stop90.

The kinetics of $M_2$ expression in 293T and MDCK cells infected with either rWSN M-Ud or rWSN M-Ud $M_2$Stop70 was then assessed. Western blots showing expression of the $M_1$ and $M_2$ proteins at 3, 6, 9, and 12 h indicate a defect in expression of the $M_2$Stop70 protein from virus-infected 293T

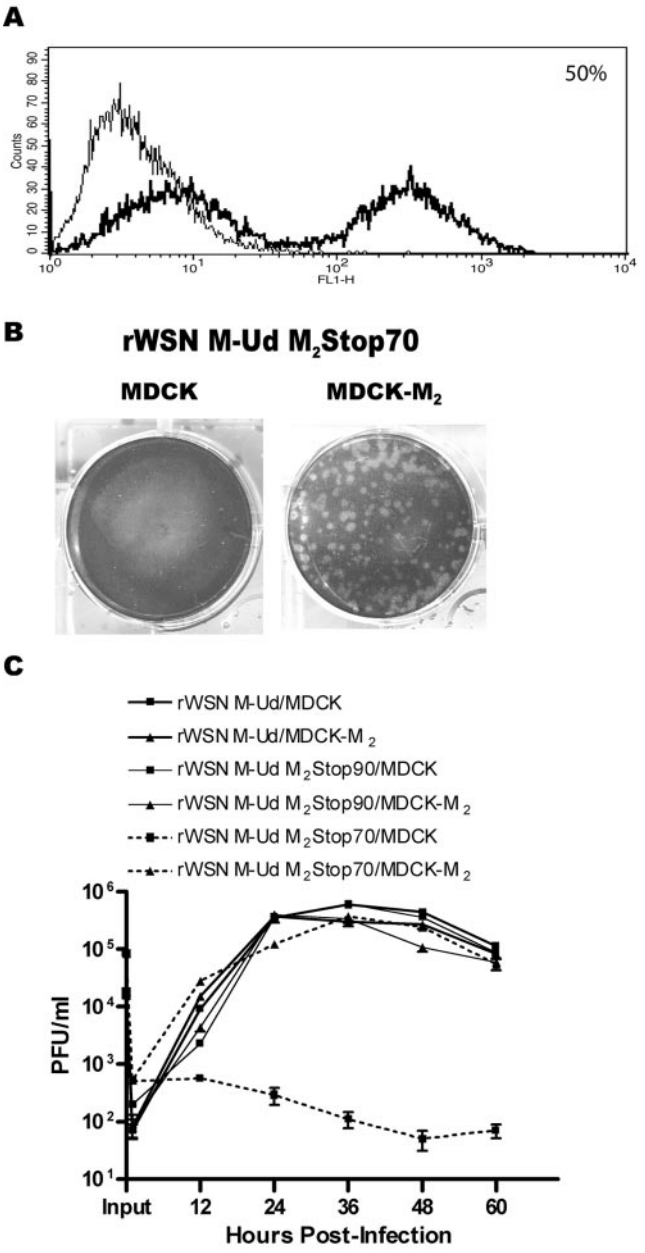


FIG. 2. Effect of $M_2$ cytoplasmic tail truncations on influenza A virus replication. (A) MDCK-$M_2$ cells were analyzed by flow cytometry for expression of the $M_2$ protein. The thin line represents cells stained with only secondary antibody, and the thick line represents cells stained with a primary antibody against $M_2$ and a fluorescein isothiocyanate-conjugated secondary antibody. (B) A plaque assay on the virus rWSN M-Ud $M_2$Stop70 was performed with MDCK and MDCK-$M_2$ cells. (C) A multistep growth curve was performed on MDCK and MDCK-$M_2$ cells with the viruses rWSN M-Ud, rWSN M-Ud $M_2$Stop90, and rWSN M-Ud $M_2$Stop70.

cells (Fig. 3B) and MDCK cells (Fig. 3C). The wild-type $M_2$ protein is first detected at 6 h postinfection and is highly expressed by 12 h postinfection in both cell types. The $M_2$Stop70 protein is barely detectable at 9 and 12 h postinfection in 293T cells and 12 h in MDCK cells. The expression of the $M_1$ and $M_2$ proteins during rWSN M-Ud, rWSN M-Ud $M_2$Stop90, and rWSN M-Ud $M_2$Stop70 infection were also examined by flow cytometry (Table 2). Although $M_1$ expression was equivalent in all virus-infected cells, the cell surface expression of both truncated $M_2$ proteins was drastically reduced compared to full-length $M_2$. Taken together, these results indicate that the $M_2$Stop70 protein was not efficiently expressed in virus-infected cells in contrast to expression from cDNA. The cell surface expression of the $M_2$Stop90 protein was significantly reduced in virus-infected cells in contrast to expression from cDNA. Since the rWSN M-Ud $M_2$Stop90 virus replicated with the same kinetics and to the same level as wild-type virus, we conclude that not only is the $M_2$Stop90 protein functional but that only a small amount of $M_2$ expression at the cell surface is required for influenza A virus replication.

**Replication of rWSN M-Ud $M_2$Stop70 in an MDCK-$M_2$Stop70 cell line.** The inability of rWSN M-Ud $M_2$Stop70 to replicate on MDCK cells (Fig. 2B) may be the consequence of low expression of the $M_2$Stop70 protein and not the result of deleting a critical domain in the cytoplasmic tail. To address this possibility, a stable cell line expressing the $M_2$Stop70 protein (MDCK-$M_2$Stop70) was generated (Fig. 3D). Approximately 57% of the cells expressed $M_2$Stop70 at the plasma membrane (mean channel fluorescence = 181) (Fig. 3D). Compared to the $M_2$-expressing cell line, this is approximately a twofold reduction in cell surface expression. A multiple-step growth curve was performed on MDCK and MDCK-$M_2$Stop70 cells with rWSN M-Ud and rWSN M-Ud $M_2$Stop70 (Fig. 3E). rWSN M-Ud replicated with similar kinetics and to a similar titer on MDCK and MDCK-$M_2$Stop70 cells. The replication of rWSN M-Ud $M_2$Stop70 was not restored by infection of MDCK-$M_2$Stop70 cells. rWSN M-Ud $M_2$Stop70 replicated to ~1,000-fold-lower levels on either cell type compared to rWSN M-Ud. These results indicate that the defect in expression of the $M_2$Stop70 protein does not account for the lack of replication of the rWSN M-Ud $M_2$Stop70 virus.

**Virion budding, morphology, and polypeptide composition.** The amount of rWSN M-Ud $M_2$Stop70 virions released from MDCK cells was reduced fourfold compared to rWSN M-Ud virions released from the same cell type (Table 3), but this effect was clearly not as dramatic as the 1,000-fold decrease in infectivity (Fig. 2C). The budding of rWSN M-Ud $M_2$Stop70 was partially restored on MDCK-$M_2$ cells, whereas infectivity was almost identical (Fig. 2B), indicating the full-length $M_2$ protein is important for efficient infectious virion production.

Next, virions were examined to determine whether there was a gross morphological difference between viruses encoding a full-length $M_2$ protein or a truncated $M_2$ protein. MDCK cells were infected with rWSN M-Ud or rWSN M-Ud $M_2$Stop70 and 15 h postinfection the virions were collected, purified, and analyzed by negative stain electron microscopy. Both rWSN M-Ud and rWSN M-Ud $M_2$Stop70 produced similar spherical virions with diameters between 80 and 120 nm (Fig. 4A), as well as filamentous virions (data not shown), indicating the $M_2$ cytoplasmic tail is not important for maintaining virion morphology.

The polypeptide composition of the purified virions was then examined. Western blotting for the $M_2$ protein demonstrates that rWSN M-Ud $M_2$Stop70 virions from infected MDCK cells do not contain a detectable amount of the $M_2$Stop70 protein;

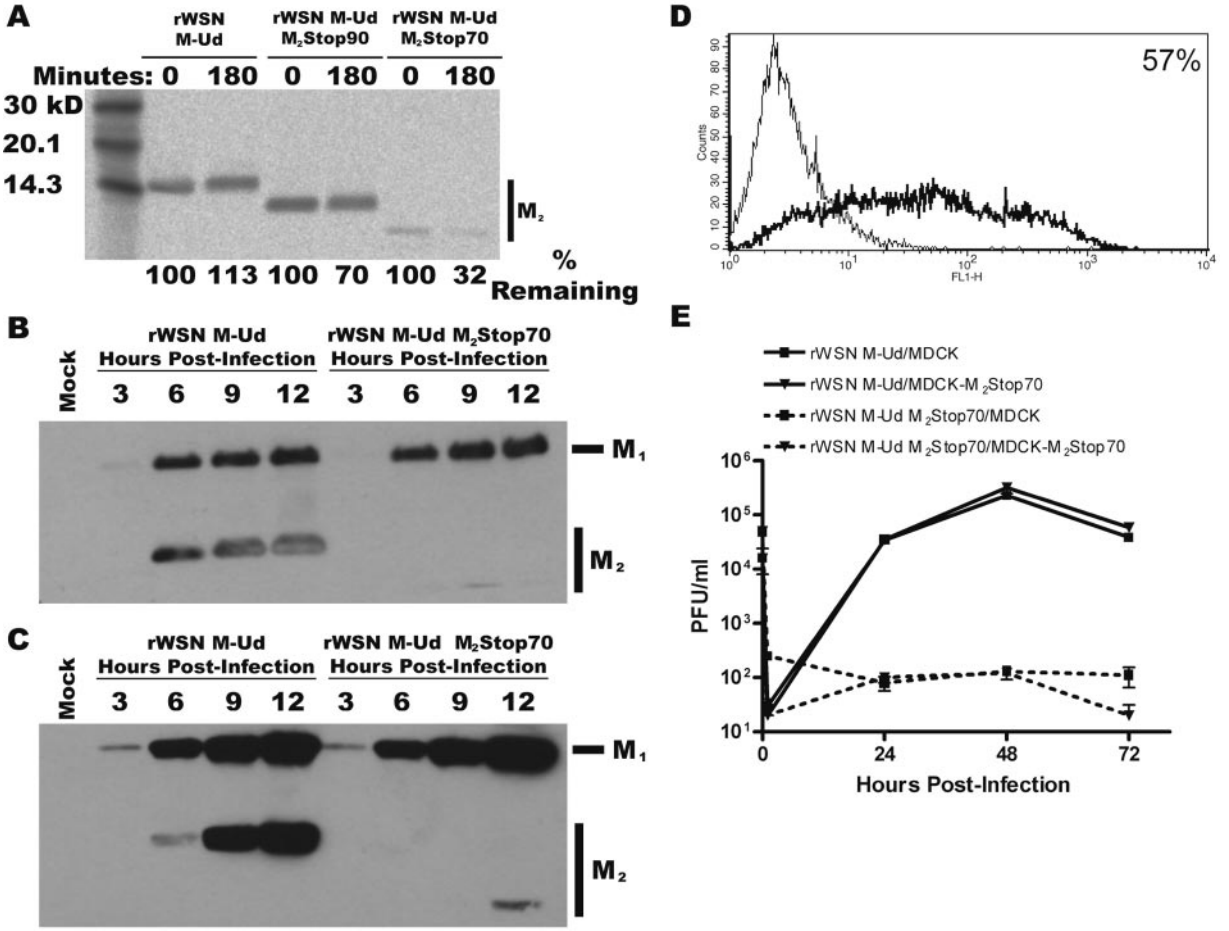


FIG. 3. The $M_2$Stop70 protein is unable to support influenza A virus replication. (A) 293T cells were infected at an MOI of 1.0 with the indicated virus and metabolically labeled, and cell lysates were immunoprecipitated with an MAb to $M_2$. The proteins were separated by SDS-PAGE and visualized with a phosphorimager. (B and C) 293T (B) or MDCK (C) cells were infected at an MOI of 1.0 with the indicated virus. At 3, 6, 9, and 12 h postinfection the cells were lysed, and the polypeptides were separated by SDS-PAGE and analyzed by Western blotting for the $M_1$ and $M_2$ proteins. (D) MDCK-$M_2$Stop70 cells were analyzed by flow cytometry for expression of the $M_2$ protein. The thin line represents cells stained with only secondary antibody, and the thick line represents cells stained with a primary antibody against $M_2$ and a fluorescein isothiocyanate-conjugated secondary antibody. (E) A multistep growth curve was performed on MDCK and MDCK-$M_2$Stop70 cells with rWSN M-Ud and rWSN M-Ud $M_2$Stop70.

this is most likely a consequence of the low level of $M_2$Stop70 protein expressed in virus-infected cells (Fig. 4B). rWSN M-Ud $M_2$Stop70 virions from infected MDCK-$M_2$ or MDCK-$M_2$Stop70 cells do incorporate the full-length and truncated $M_2$ protein expressed in *trans*, indicating the $M_2$Stop70 protein can be incorporated into virus particles in a manner similar to full-length $M_2$ (Fig. 4B). The $M_2$Stop70 protein can also be incorporated into rWSN M-Ud virions grown on MDCK-$M_2$Stop70 cells without any apparent detrimental effects on virus infectivity. These data indicate that the C-terminal 28 amino acids of $M_2$ are not required for $M_2$ incorporation into virus particles, that incorporation of $M_2$Stop70 protein into virus particles does not restore rWSN M-Ud $M_2$Stop70 infectivity, and that inclusion of $M_2$Stop70 into wild-type virions does not alter their infectivity.

TABLE 3. Decreased total virion production from MDCK cells infected with virus encoding a truncated $M_2$ protein

| Virus | Cells (HA U/ml)[a] | |
|---|---|---|
| | MDCK | MDCK-$M_2$ |
| rWSN M-Ud | 1,280 | 1,280 |
| rWSN M-Ud $M_2$Stop70 | 320 | 640 |

[a] The indicated cells were infected at an MOI of 1.0 in duplicate, and then 12 h postinfection HA assays were performed (also in duplicate).

The virion polypeptide composition was then examined to determine whether incorporation of other viral proteins was altered in the presence of cytoplasmic tail-truncated $M_2$. Virions from rWSN M-Ud or rWSN M-Ud $M_2$Stop70-infected MDCK, MDCK-$M_2$, and MDCK-$M_2$Stop70 cells were purified, and equivalent numbers of virus particles (as judged by Western blotting for HA protein) were analyzed for HA, $M_1$, and NP incorporation (Fig. 4C). Levels of HA and $M_1$ were similar in all virions regardless of the cell type used to generate the virus particles. In contrast, NP incorporation was reduced in the rWSN M-Ud $M_2$Stop70 virions purified from infected

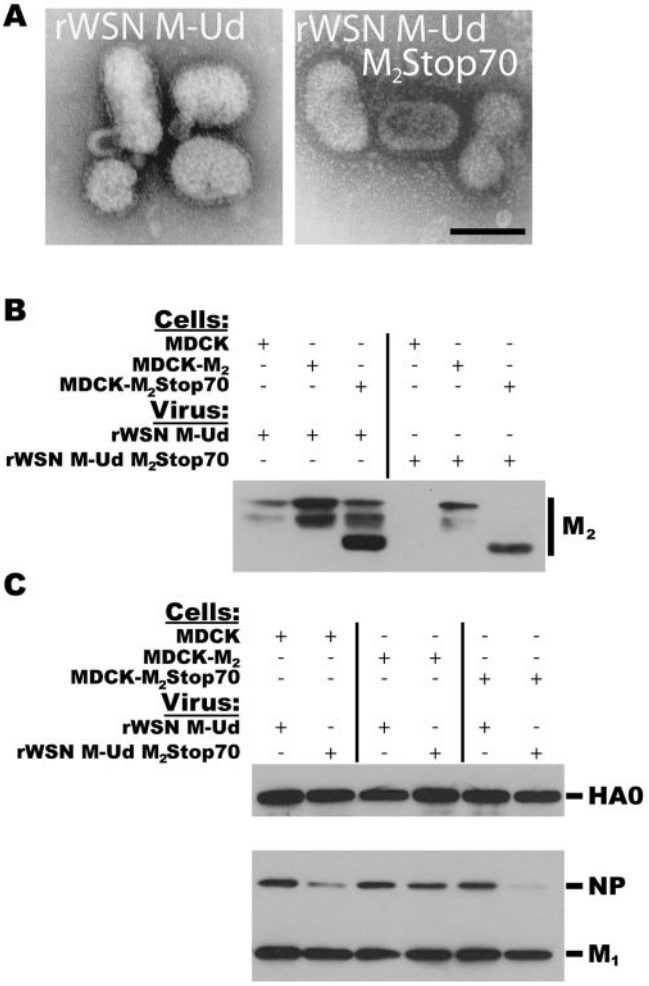


FIG. 4. The effect of $M_2$ protein *trans*-complementation on rWSN M-Udorn $M_2$Stop70 virus morphology and polypeptide composition. (A) Purified virions were negatively stained with uranyl acetate and examined with a JEOL 1200EX transmission electron microscope. Scale bar, 100 nm. (B and C) Purified virions from MDCK, MDCK-$M_2$, and MDCK-$M_2$Stop70 infected cells were analyzed by Western blotting. In panel B an MAb to $M_2$ was used, and in panel C antibodies to HA, NP, and $M_1$ were used. The band migrating slightly faster than full-length $M_2$ is a proteolytic fragment of $M_2$.

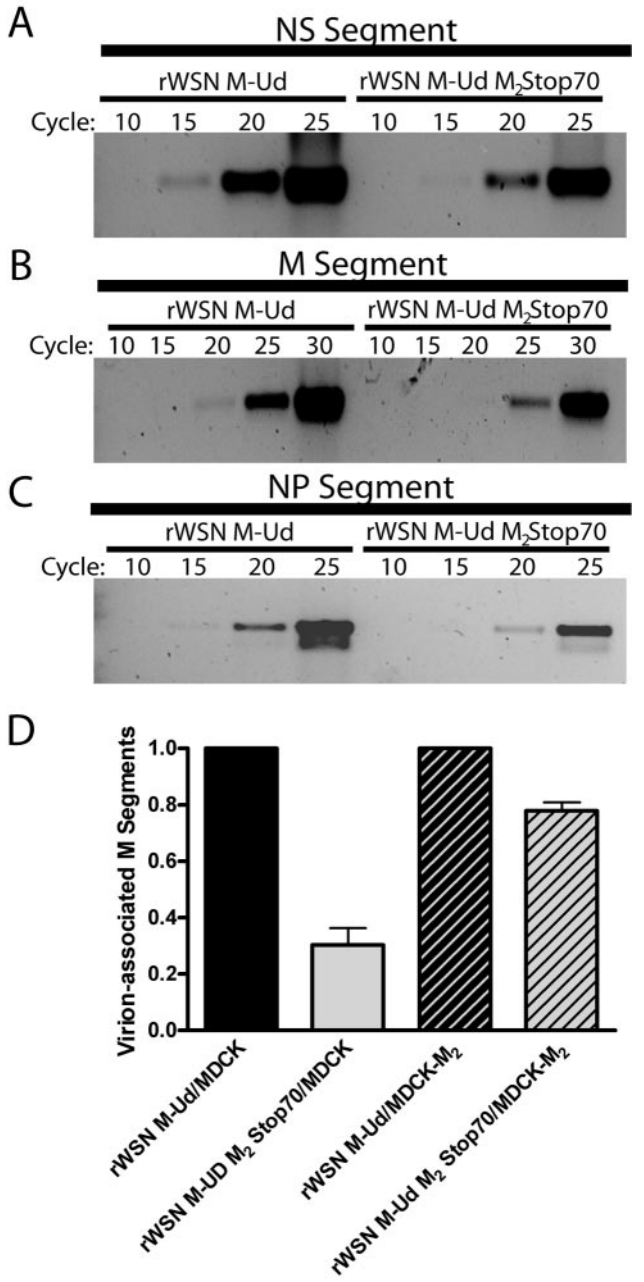


FIG. 5. RNA incorporation into rWSN M-Ud and rWSN M-Ud $M_2$Stop70 virions. RNA was extracted from the indicated virions, and a semiquantitative RT-PCR was performed with primers specific for the NS segment (A), the M segment (B), and the NP segment (C). (D) RNA was extracted from the indicated virions, reverse transcribed with primers specific for the M segment, and quantitated by real-time PCR.

MDCK or MDCK-$M_2$Stop70 cells. NP incorporation was restored to near wild-type levels in rWSN M-Ud $M_2$Stop70 virions harvested from MDCK-$M_2$ cells. Thus, the data suggest that $M_2$ cytoplasmic tail truncations can alter the efficiency of NP, but not HA or $M_1$, incorporation into influenza virions and that full-length $M_2$ protein expressed in *trans* can complement this defect. The data also suggest that $M_2$ packaging is independent of NP packaging, since overexpression of $M_2$Stop70 resulted in increased $M_2$ incorporation into virions (Fig. 4B) without altering the amount of NP in the particles (Fig. 4C).

**RNA incorporation into virions.** The reduced infectivity and decreased NP incorporation into virions with truncated $M_2$ proteins suggested that vRNP packaging was somehow reduced. To test this hypothesis, MDCK cells were infected with rWSN M-Ud or rWSN M-Ud $M_2$Stop70, the virions were collected 15 h postinfection, and RNA was extracted from equivalent numbers of virus particles as judged by hemagglutination of chicken red blood cells. RT-PCR with primers specific for the influenza A virus NS, M, or NP segments was performed, and the reactions were sampled at the indicated cycles. There were reduced amounts of all three RNA segments in rWSN M-Ud $M_2$Stop70 virions compared to rWSN M-Ud virions (Fig. 5A to C). In order to determine whether complementa-

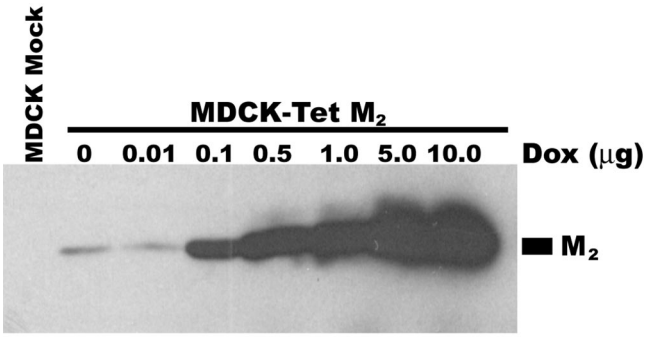


FIG. 6. Characterization of MDCK cells with inducible $M_2$ expression. MDCK-Tet $M_2$ cells were incubated in the absence or presence of increasing concentrations of doxycycline for 48 h. At 48 h the cells were lysed, the polypeptides were separated by SDS-PAGE and analyzed by Western blotting with an antibody to the $M_2$ protein.

tion with the full-length $M_2$ protein would restore genome incorporation, RNA was extracted from virions derived from infected MDCK or MDCK-$M_2$ cells, and M segment RNA was quantitated by real-time RT-PCR (Fig. 5D). There was an ~3.3-fold reduction in M segment incorporated in rWSN M-Ud $M_2$Stop70 virions from MDCK cells but only a 1.3-fold reduction in rWSN M-Ud $M_2$Stop70 virions from MDCK-$M_2$ cells. These results indicate that truncations in the $M_2$ cytoplasmic tail result in reduced RNA incorporation into progeny virus particles and that expression of the full-length $M_2$ protein in *trans* is sufficient to restore RNA incorporation.

**Growth of rWSN M-Ud $M_2$Stop70 on an inducible $M_2$ expression cell line.** We sought to determine the amount of $M_2$ expression needed to restore rWSN M-Ud $M_2$Stop70 virus replication to wild-type levels. A tetracycline-inducible MDCK cell line (MDCK-Tet$M_2$) was established, and Western blotting for $M_2$ expression shows a low basal level of $M_2$ expression, as well as high levels of doxycycline-inducible $M_2$ expression (Fig. 6). The amount of $M_2$ protein needed to restore replication of rWSN M-Ud $M_2$Stop70 was examined by infecting MDCK-Tet$M_2$ cells in the presence or absence of 1 μg of doxycycline/ml. The basal expression of $M_2$ from MDCK-Tet$M_2$ cells was sufficient to increase the replication of rWSN M-Ud $M_2$Stop70 ca. 10,000-fold, which is nearly identical to the findings with wild-type virus (Table 4). We therefore conclude that only a very small amount of $M_2$ expression is required for efficient influenza A virus replication. This is consistent with our observations of low levels of M2Stop90 at the cell surface of rWSN M-Ud $M_2$Stop90 virus (Table 2) being sufficient to confer wild-type replication kinetics to the virus (Fig. 2C).

TABLE 4. Restoration of $M_2$ truncated + virus replication on MDCK cells with tetracycline-inducible $M_2$ expression

| Virus | $TCID_{50}$ | | |
|---|---|---|---|
| | MDCK | MDCK Tet-$M_2$ | MDCK Tet-$M_2$ + 1 μg of Dox/ml[a] |
| rWSN M-Ud | $1.44 \times 10^6$ | $3.30 \times 10^6$ | $7.24 \times 10^5$ |
| rWSN M-Ud $M_2$Stop70 | $4.21 \times 10^2$ | $4.22 \times 10^6$ | $1.47 \times 10^7$ |

[a] Dox, doxycycline.

**Generation of revertant viruses during rWSN M-Ud $M_2$Stop70 infection.** When the multiple-step growth curves were prepared, we noticed that the titer for certain rWSN M-Ud $M_2$Stop70 replicates began increasing late in infection. One 72-h time point was analyzed by plaque assay on MDCK cells, and virus plaques were clearly visible (data not shown), in contrast to the lack of plaque formation seen with rWSN M-Ud $M_2$Stop70 viruses (Fig. 2B). Ten individual plaques were picked, and the M segment genomic sequence was determined by RT-PCR and sequencing. Table 1 shows the sequence of rWSN M-Ud $M_2$Stop70 revertants. The stop codons at position 70 and 71 were altered to encode for tryptophans in all 10 revertant viruses sequenced. These mutations allowed for read through and expression of the full-length $M_2$ protein. Expression of the full-length $M_2$ protein was confirmed by Western blotting of virus-infected cell lysates with an MAb specific for the $M_2$ protein (Fig. 7A). Additional mutations in the $M_2$ cytoplasmic tail and in the $M_1$ protein were detected, but these were only present in a subset of the 10 revertant viruses sequenced. To determine whether the mutations present in the rWSN M-Ud $M_2$Stop70 revertant allowed for this virus to efficiently replicate on MDCK cells, a multiple-step growth curve was performed on MDCK cells with rWSN M-Ud, rWSN M-Ud $M_2$Stop70, and rWSN M-Ud $M_2$Stop70 revertant (Fig. 7B). The replication of rWSN M-Ud $M_2$Stop70 revertant was equivalent to, or slightly higher, than rWSN M-Ud. The isolation of rWSN M-Ud $M_2$Stop70 revertants indicates the strong selection pressure for maintaining expression of the full-length cytoplasmic tail of the $M_2$ protein.

## DISCUSSION

The process of enveloped virion assembly involves multiple interactions between viral proteins, host proteins, the viral genome, and host lipids. A successful outcome results in the release of a viral particle that has incorporated the correct complement of protein and genetic material that will allow for a neighboring cell, or host, to become infected. For influenza A virus, this entails the incorporation of the three integral membrane proteins HA, NA, and $M_2$ and the eight RNA segments, in the form of RNP complexes, that comprise the influenza A virus genome (29). In the present study, we attempted to define the role of the cytoplasmic tail of the $M_2$ protein in influenza A virus replication and determined that the cytoplasmic tail is critical for the assembly of infectious virus particles.

The cytoplasmic tail of the $M_2$ protein is predicted to contain 54 amino acids (31). In order to examine the role it may play in influenza A virus replication, we generated recombinant viruses encoding $M_2$ proteins with truncations in the cytoplasmic tail. $M_2$ is a type III integral membrane protein that requires the presence of a portion of the cytoplasmic tail in order for the hydrophobic transmembrane domain to be recognized by the signal recognition particle and translocated into to the endoplasmic reticulum membrane (25, 31, 67). We confirmed that the $M_2$ truncation proteins were still transported to the cell surface appropriately when expressed from cDNA, a finding in agreement with the published literature (57). In addition, we confirmed that the ion channel activity of

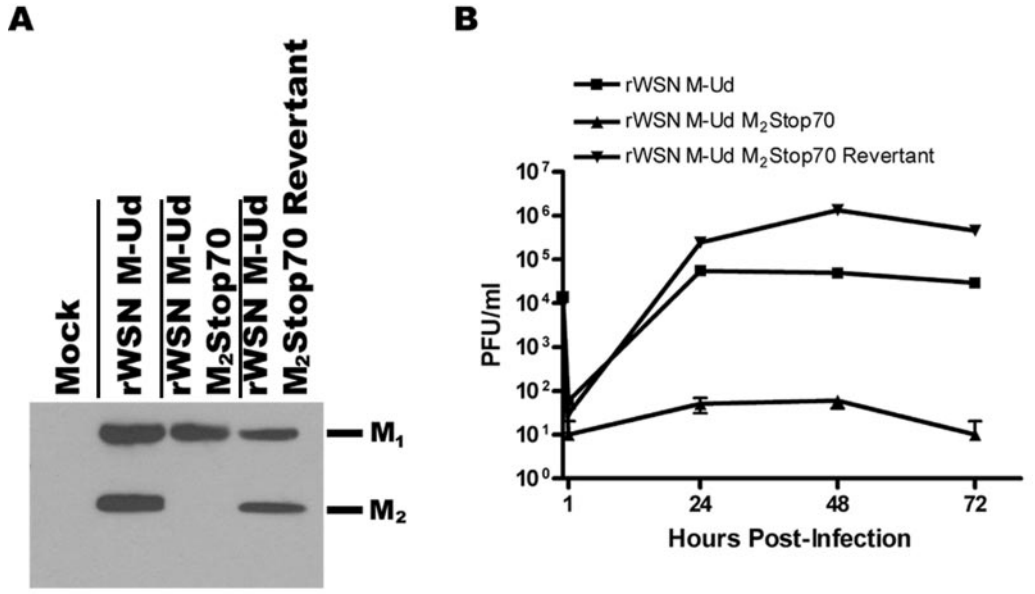


FIG. 7. Analysis of rWSN M-Ud $M_2$Stop70 Revertant. (A) Western blot of virus-infected cell lysates with MAbs to $M_2$ and $M_1$. (B) A multistep growth curve was performed on MDCK cells infected with rWSN M-Ud, rWSN M-Ud $M_2$Stop70, or rWSN M-Ud $M_2$Stop70 revertant.

$M_2$Stop70 protein was not compromised by using a functional assay based on the transport of FPV HA. Our data on the ion channel activity of $M_2$Stop70 is consistent with Tobler et al. (57), who demonstrated that $M_2$ proteins with comparable cytoplasmic tail deletions have wild-type ion channel activities when expressed in *Xenopus laevis* oocytes.

The replication of rWSN M-Ud $M_2$Stop90 and rWSN M-Ud $M_2$Stop70 on MDCK cells demonstrated the requirement for amino acids 70 to 89 in the $M_2$ protein. rWSN M-Ud $M_2$Stop70 does not express the $M_2$Stop70 protein to a high level for an undetermined reason. Replication levels were restored when the virus was grown on a cell line stably expressing full-length $M_2$ and not on one expressing $M_2$Stop70. Only when adaptive mutations allowing for the expression of full-length $M_2$ were acquired did the virus replicate to wild-type levels on MDCK cells. A similar defect in replication is observed when the $M_2$ protein is truncated in viruses bearing all eight segments from either the WSN or Udorn genetic background (data not shown), suggesting that the defect in virus replication resulting from $M_2$ cytoplasmic tail deletion is not peculiar to the reassortant viruses we analyzed here.

The requirements for amino acids 70 to 89 in the cytoplasmic tail of $M_2$ provide evidence that a potential $M_2$-$M_1$ interaction is essential for influenza A virus replication by mediating efficient packaging of vRNPs. The reduced replication of A/Udorn/72, in the presence of the anti-$M_2$ MAb 14C2, allowed for antibody-resistant variants to be isolated (64, 65). Antibody epitope escape mutants were found rarely, but mutations that restored replication without altering antibody binding were identified. Interestingly, single amino acid substitutions at residue 71 or 78 in the $M_2$ cytoplasmic tail were isolated (66) in addition to mutations at position 31 and 41 of the $M_1$ protein. The one mutation in the $M_1$ protein, an Ala-to-Thr change at position 22, identified in two plaque-purified rWSN $M_2$Stop70 revertant viruses is located proximally to amino acids 31 and 41 in the $M_1$ crystallographic structure (1, 17). These antibody-resistant variants, together with viruses with the $M_2$ cytoplasmic tail deleted, provide genetic evidence for a potential interaction between the $M_2$ and $M_1$ proteins during influenza A virus assembly. Studies designed to detect a direct physical interaction between $M_2$ and $M_1$ and how mutations in the $M_1$ protein may influence this interaction are currently being pursued.

The major defect in replication of rWSN M-Ud $M_2$Stop70 on MDCK cells was decreased levels of NP and genomic RNA incorporation into virions. As a result of this defect, rWSN M-Ud $M_2$Stop70 virions released from MDCK cells demonstrated a lower ability to replicate compared to rWSN M-Ud. This defect was not seen when $M_2$ was provided in *trans*, indicating that it was a result of altered protein function and not a consequence of altering the nucleotide sequence of the M segment RNA. In addition, MDCK cells produced fewer virions when infected with rWSN M-Ud $M_2$Stop70 than rWSN M-Ud, although this defect in virus particle assembly (4-fold decrease) was not nearly as great as the defect in infectivity (1,000-fold). These results provide us with evidence to present a model in which the $M_2$ cytoplasmic tail interacts with $M_1$-RNP complexes leading to genome incorporation into budding virions. The incorporation of $M_2$ into virus particles is independent of this interaction, since $M_2$Stop70 protein can be efficiently incorporated into virus particles with no apparent change in NP or RNP packaging. Curiously, reductions in the amount of $M_1$ packaged into rWSN M-Ud $M_2$Stop70 virions were not seen. This is most likely due to the fact that the majority of virion-associated $M_1$ is packaged through interactions with the HA and NA cytoplasmic tails and/or membrane interactions and therefore is not associated with RNPs. The RNP-associated $M_1$ is only a small fraction of the total packaged $M_1$, and the loss of this small amount of $M_1$ is not detectable using our assays.

Influenza A virus particles can package vRNPs either specifically—through segment-specific packaging signals in noncoding (11) and coding regions (12, 62)—or nonspecifically (2, 10, 33). We hypothesize that the reduced packaging of vRNPs seen in rWSN M-Ud $M_2$Stop70 particles is a result of decreased specific vRNP packaging mediated by amino acids 70 to 89 of the $M_2$ cytoplasmic tail, although we cannot rule out the possibility that the $M_2$ cytoplasmic tail is responsible for selecting only a subset of vRNPs for virion packaging. Genome packaging was detected in rWSN M-Ud $M_2$Stop70 virions, implying $M_2$ is not absolutely essential for vRNP incorporation. However, the $M_2$ protein, through its cytoplasmic tail, may facilitate virion incorporation of a full genomic complement of vRNPs, thereby making the production of an infectious virus particle more likely. Our study showed that at least three genomic RNA segments (NS, M, and NP) were reduced in rWSN M-Ud $M_2$Stop70 virions; we are currently investigating whether all RNA segments are reduced.

The $M_2$ protein is expressed abundantly at the cell surface; however, it is only a minor component of influenza A virions (31, 65). We attempted to quantify the amount of $M_2$ needed to restore replication to rWSN M-Ud $M_2$Stop70 viruses by using a cell line capable of expressing $M_2$ in a tetracycline-inducible manner. The results presented here suggest that even low-level expression of wild-type $M_2$, through leakiness in the Tet-On system, provides enough $M_2$ to restore replication to near wild-type levels. In addition, the low cell surface expression of $M_2$Stop90 in virus-infected cells was not detrimental to replication since this virus was indistinguishable from wild-type virus with respect to the kinetics and extent of infectious virus production.

Watanabe et al. characterized the replication of a recombinant influenza A virus bearing a deletion of the transmembrane and cytoplasmic domains of the $M_2$ protein (61). This virus had the same genetic background (seven segments from WSN and M segment from Udorn) as our $M_2$-truncated viruses, formed pinpoint plaques, and was able to grow to significant titers at late times postinfection. Of particular relevance, the virus in that study was genetically stable for 10 passages in tissue culture. Our cytoplasmic tail-truncated viruses did not plaque efficiently, and we found a much higher tendency for reversions, suggesting a strong selection pressure for restoring the full-length $M_2$ cytoplasmic tail. Since the lack of $M_2$Stop70 protein expression in virus-infected cells effectively makes this an $M_2$ deletion virus, it is unclear to us why our data differs from that of Watanabe et al.

Other viruses in the *Orthomyxoviridae* family encode small integral membrane proteins that appear analogous to the influenza A virus $M_2$ protein. Influenza C virus encodes an integral membrane protein CM2, which forms tetramers (46, 48) and has reported ion channel activity (22). In addition, recent evidence clearly demonstrates that the BM2 protein of influenza B virus is the functional homolog of $M_2$ with respect to ion channel activity (39). The BM2 protein is an integral membrane protein that forms a tetramer when expressed in virus-infected or cDNA-transfected cells (45, 60). Of particular interest is the finding that the recombinant influenza B viruses bearing deletions or alterations in the BM2 coding sequence only replicate efficiently if wild-type BM2 is provide in *trans* (18, 27). In fact, a role for BM2 in influenza B virus RNP packaging has recently been suggested (26), lending further support to our hypothesis. It is interesting to speculate that in addition to providing ion channel activity that is important for efficient release of genomic RNA segments during viral entry, $M_2$, BM2, and CM2 may also play a role in packaging viral genomic segments.

## ACKNOWLEDGMENTS

We thank Yoshi Kawaoka for the plasmids encoding the A/WSN/33 infectious clone; Robert Lamb for the 14C2 MAb, the anti-FPV HA sera, and the FPV HA cDNA; and all of the members of the Pekosz lab for critical discussions.

This study was supported by grant AI053629 from the Department of Health and Human Services and a Whitaker Foundation Young Investigator Award (both to A.P.). M.F.M. was supported by grant T32 AI07172 from the Department of Health and Human Services.

## REFERENCES

1. **Arzt, S., F. Baudin, A. Barge, P. Timmins, W. P. Burmeister, and R. W. H. Ruigrok.** 2001. Combined results from solution studies on intact influenza virus M1 protein and from a new crystal form of its N-terminal domain show that M1 is an elongated monomer. Virology **279:**439–446.
2. **Bancroft, C. T., and T. G. Parslow.** 2002. Evidence for segment-nonspecific packaging of the influenza a virus genome. J. Virol. **76:**7133–7139.
3. **Barman, S., L. Adhikary, A. K. Chakrabarti, C. Bernas, Y. Kawaoka, and D. P. Nayak.** 2004. Role of transmembrane domain and cytoplasmic tail amino acid sequences of influenza A virus neuraminidase in raft association and virus budding. J. Virol. **78:**5258–5269.
4. **Bukrinskaya, A. G., N. K. Vorkunova, G. V. Kornilayeva, R. A. Narmanbetova, and G. K. Vorkunova.** 1982. Influenza virus uncoating in infected cells and effect of rimantadine. J. Gen. Virol. **60:**49–59.
5. **Bukrinskaya, A. G., N. K. Vorkunova, and N. L. Pushkarskaya.** 1982. Uncoating of a rimantadine-resistant variant of influenza virus in the presence of rimantadine. J. Gen. Virol. **60:**61–66.
6. **Chizhmakov, I. V., F. M. Geraghty, D. C. Ogden, A. Hayhurst, M. Antoniou, and A. J. Hay.** 1996. Selective proton permeability and pH regulation of the influenza virus M2 channel expressed in mouse erythroleukaemia cells. J. Physiol. **494**(Pt. 2)**:**329–336.
7. **Ciampor, F., P. M. Bayley, M. V. Nermut, E. M. Hirst, R. J. Sugrue, and A. J. Hay.** 1992. Evidence that the amantadine-induced, M2-mediated conversion of influenza A virus hemagglutinin to the low pH conformation occurs in an acidic *trans*-Golgi compartment. Virology **188:**14–24.
8. **Ciampor, F., C. A. Thompson, S. Grambas, and A. J. Hay.** 1992. Regulation of pH by the M2 protein of influenza A viruses. Virus Res. **22:**247–258.
9. **Duff, K. C., and R. H. Ashley.** 1992. The transmembrane domain of influenza A M2 protein forms amantadine-sensitive proton channels in planar lipid bilayers. Virology **190:**485–489.
10. **Enami, M., G. Sharma, C. Benham, and P. Palese.** 1991. An influenza virus containing nine different RNA segments. Virology **185:**291–298.
11. **Flandorfer, A., A. Garcia-Sastre, C. F. Basler, and P. Palese.** 2003. Chimeric influenza A viruses with a functional influenza B virus neuraminidase or hemagglutinin. J. Virol. **77:**9116–9123.
12. **Fujii, Y., H. Goto, T. Watanabe, T. Yoshida, and Y. Kawaoka.** 2003. Selective incorporation of influenza virus RNA segments into virions. Proc. Natl. Acad. Sci. USA **100:**2002–2007.
13. **Gomez-Puertas, P., C. Albo, E. Perez-Pastrana, A. Vivo, and A. Portela.** 2000. Influenza virus matrix protein is the major driving force in virus budding. J. Virol. **74:**11538–11547.
14. **Gomez-Puertas, P., I. Mena, M. Castillo, A. Vivo, E. Perez-Pastrana, and A. Portela.** 1999. Efficient formation of influenza virus-like particles: dependence on the expression levels of viral proteins. J. Gen. Virol. **80**(Pt. 7)**:** 1635–1645.
15. **Grambas, S., M. S. Bennett, and A. J. Hay.** 1992. Influence of amantadine resistance mutations on the pH regulatory function of the M2 protein of influenza A viruses. Virology **191:**541–549.
16. **Griffin, S. D., R. Harvey, D. S. Clarke, W. S. Barclay, M. Harris, and D. J. Rowlands.** 2004. A conserved basic loop in hepatitis C virus p7 protein is required for amantadine-sensitive ion channel activity in mammalian cells but is dispensable for localization to mitochondria. J. Gen. Virol. **85:**451–461.
17. **Harris, A., F. Forouhar, S. Qiu, B. Sha, and M. Luo.** 2001. The crystal structure of the influenza matrix protein M1 at neutral pH: M1–M1 protein interfaces can rotate in the oligomeric structures of M1. Virology **289:**34–44.
18. **Hatta, M., H. Goto, and Y. Kawaoka.** 2004. Influenza B virus requires BM2 protein for replication. J. Virol. **78:**5576–5583.
19. **Hay, A. J., A. J. Wolstenholme, J. J. Skehel, and M. H. Smith.** 1985. The molecular basis of the specific anti-influenza action of amantadine. EMBO J. **4:**3021–3024.

20. **Henkel, J. R., and O. A. Weisz.** 1998. Influenza virus M2 protein slows traffic along the secretory pathway: pH perturbation of acidified compartments affects early Golgi transport steps. J. Biol. Chem. **273:**6518–6524.
21. **Holsinger, L. J., and R. A. Lamb.** 1991. Influenza virus M2 integral membrane protein is a homotetramer stabilized by formation of disulfide bonds. Virology **183:**32–43.
22. **Hongo, S., K. Ishii, K. Mori, E. Takashita, Y. Muraki, Y. Matsuzaki, and K. Sugawara.** 2004. Detection of ion channel activity in *Xenopus laevis* oocytes expressing Influenza C virus CM2 protein. Arch. Virol. **149:**35–50.
23. **Huang, T. S., P. Palese, and M. Krystal.** 1990. Determination of influenza virus proteins required for genome replication. J. Virol. **64:**5669–5673.
24. **Hughey, P. G., P. C. Roberts, L. J. Holsinger, S. L. Zebedee, R. A. Lamb, and R. W. Compans.** 1995. Effects of antibody to the influenza A virus M2 protein on M2 surface expression and virus assembly. Virology **212:**411–421.
25. **Hull, J. D., R. Gilmore, and R. A. Lamb.** 1988. Integration of a small integral membrane protein, M2, of influenza virus into the endoplasmic reticulum: analysis of the internal signal-anchor domain of a protein with an ectoplasmic $NH_2$ terminus. J. Cell Biol. **106:**1489–1498.
26. **Imai, M., S. Watanabe, A. Ninomiya, M. Obuchi, and T. Odagiri.** 2004. Influenza B virus BM2 protein is a crucial component for incorporation of viral ribonucleoprotein complex into virions during virus assembly. J. Virol. **78:**11007–11015.
27. **Jackson, D., T. Zurcher, and W. Barclay.** 2004. Reduced incorporation of the influenza B virus BM2 protein in virus particles decreases infectivity. Virology **322:**276–285.
28. **Jin, H., G. P. Leser, J. Zhang, and R. A. Lamb.** 1997. Influenza virus hemagglutinin and neuraminidase cytoplasmic tails control particle shape. EMBO J. **16:**1236–1247.
29. **Lamb, R. A., and R. M. Krug.** 2001. Orthomyxoviridae: the viruses and their replication, p. 1487–1532. *In* D. M. Knipe and P. M. Howley (ed.), Fields virology. Lippincott/The Williams & Wilkins Co., Philadelphia, Pa.
30. **Lamb, R. A., C. J. Lai, and P. W. Choppin.** 1981. Sequences of mRNAs derived from genome RNA segment 7 of influenza virus: colinear and interrupted mRNAs code for overlapping proteins. Proc. Natl. Acad. Sci. USA **78:**4170–4174.
31. **Lamb, R. A., S. L. Zebedee, and C. D. Richardson.** 1985. Influenza virus M2 protein is an integral membrane protein expressed on the infected-cell surface. Cell **40:**627–633.
32. **Latham, T., and J. M. Galarza.** 2001. Formation of wild-type and chimeric influenza virus-like particles following simultaneous expression of only four structural proteins. J. Virol. **75:**6154–6165.
33. **Luytjes, W., M. Krystal, M. Enami, J. D. Pavin, and P. Palese.** 1989. Amplification, expression, and packaging of foreign gene by influenza virus. Cell **59:**1107–1113.
34. **Martin, K., and A. Helenius.** 1991. Nuclear transport of influenza virus ribonucleoproteins: the viral matrix protein (M1) promotes export and inhibits import. Cell **67:**117–130.
35. **Martin, K., and A. Helenius.** 1991. Transport of incoming influenza virus nucleocapsids into the nucleus. J. Virol. **65:**232–244.
36. **McCown, M., M. S. Diamond, and A. Pekosz.** 2003. The utility of siRNA transcripts produced by RNA polymerase i in downregulating viral gene expression and replication of negative- and positive-strand RNA viruses. Virology **313:**514–524.
37. **Mould, J. A., J. E. Drury, S. M. Frings, U. B. Kaupp, A. Pekosz, R. A. Lamb, and L. H. Pinto.** 2000. Permeation and activation of the M2 ion channel of influenza A virus. J. Biol. Chem. **275:**31038–31050.
38. **Mould, J. A., H. C. Li, C. S. Dudlak, J. D. Lear, A. Pekosz, R. A. Lamb, and L. H. Pinto.** 2000. Mechanism for proton conduction of the $M_2$ ion channel of influenza A virus. J. Biol. Chem. **275:**8592–8599.
39. **Mould, J. A., R. G. Paterson, M. Takeda, Y. Ohigashi, P. Venkataraman, R. A. Lamb, and L. H. Pinto.** 2003. Influenza B virus BM2 protein has ion channel activity that conducts protons across membranes. Dev. Cell **5:**175–184.
40. **Neumann, G., T. Watanabe, H. Ito, S. Watanabe, H. Goto, P. Gao, M. Hughes, D. R. Perez, R. Donis, E. Hoffmann, G. Hobom, and Y. Kawaoka.** 1999. Generation of influenza A viruses entirely from cloned cDNAs. Proc. Natl. Acad. Sci. USA **96:**9345–9350.
41. **Neumann, G., T. Watanabe, and Y. Kawaoka.** 2000. Plasmid-driven formation of influenza virus-like particles. J. Virol. **74:**547–551.
42. **Niwa, H., K. Yamamura, and J. Miyazaki.** 1991. Efficient selection for high-expression transfectants with a novel eukaryotic vector. Gene **108:**193–199.
43. **Ohuchi, M., A. Cramer, M. Vey, R. Ohuchi, W. Garten, and H. D. Klenk.** 1994. Rescue of vector-expressed fowl plague virus hemagglutinin in biologically active form by acidotropic agents and coexpressed M2 protein. J. Virol. **68:**920–926.
44. **Paterson, R. G., and R. A. Lamb.** 1993. The molecular biology of influenza viruses and paramyxoviruses, p. 35–73. *In* Molecular virology: a practical approach. Oxford University Press, Oxford, United Kingdom.
45. **Paterson, R. G., M. Takeda, Y. Ohigashi, L. H. Pinto, and R. A. Lamb.** 2003. Influenza B virus BM2 protein is an oligomeric integral membrane protein expressed at the cell surface. Virology **306:**7–17.
46. **Pekosz, A., and R. A. Lamb.** 1997. The CM2 protein of influenza C virus is an oligomeric integral membrane glycoprotein structurally analogous to influenza A virus M2 and influenza B virus NB proteins. Virology **237:**439–451.
47. **Pekosz, A., and R. A. Lamb.** 2000. Identification of a membrane targeting and degradation signal in the p42 protein of influenza C virus. J. Virol. **74:**10480–10488.
48. **Pekosz, A., and R. A. Lamb.** 1998. Influenza C virus CM2 integral membrane glycoprotein is produced from a polypeptide precursor by cleavage of an internal signal sequence. Proc. Natl. Acad. Sci. USA **95:**13233–13238.
49. **Pinto, L. H., L. J. Holsinger, and R. A. Lamb.** 1992. Influenza virus M2 protein has ion channel activity. Cell **69:**517–528.
50. **Reed, L. J., and H. Muench.** 1938. A simple method of estimating 50 percent endpoints. Am. J. Hyg. **27:**493–499.
51. **Roberts, P. C., R. A. Lamb, and R. W. Compans.** 1998. The M1 and M2 proteins of influenza A virus are important determinants in filamentous particle formation. Virology **240:**127–137.
52. **Sakaguchi, T., G. P. Leser, and R. A. Lamb.** 1996. The ion channel activity of the influenza virus M2 protein affects transport through the Golgi apparatus. J. Cell Biol. **133:**733–747.
53. **Skehel, J. J., A. J. Hay, and J. A. Armstrong.** 1978. On the mechanism of inhibition of influenza virus replication by amantadine hydrochloride. J. Gen. Virol. **38:**97–110.
54. **Takeda, M., G. P. Leser, C. J. Russell, and R. A. Lamb.** 2003. Influenza virus hemagglutinin concentrates in lipid raft microdomains for efficient viral fusion. Proc. Natl. Acad. Sci. USA **100:**14610–14617.
55. **Takeda, M., A. Pekosz, K. Shuck, L. H. Pinto, and R. A. Lamb.** 2002. Influenza A virus $M_2$ ion channel activity is essential for efficient replication in tissue culture. J. Virol. **76:**1391–1399.
56. **Takeuchi, K., and R. Lamb.** 1994. Influenza virus M2 protein ion channel activity stabilizes the native form of fowl plague virus hemagglutinin during intracellular transport. J. Virol. **68:**911–919.
57. **Tobler, K., M. L. Kelly, L. H. Pinto, and R. A. Lamb.** 1999. Effect of cytoplasmic tail truncations on the activity of the M2 ion channel of influenza A virus. J. Virol. **73:**9695–9701.
58. **Wang, C., K. Takeuchi, L. H. Pinto, and R. A. Lamb.** 1993. Ion channel activity of influenza A virus M2 protein: characterization of the amantadine block. J. Virol. **67:**5585–5594.
59. **Ward, C. L., M. H. Dempsey, C. J. Ring, R. E. Kempson, L. Zhang, D. Gor, B. W. Snowden, and M. Tisdale.** 2004. Design and performance testing of quantitative real-time PCR assays for influenza A and B viral load measurement. J. Clin. Virol. **29:**179–188.
60. **Watanabe, S., M. Imai, Y. Ohara, and T. Odagiri.** 2003. Influenza B virus BM2 protein is transported through the *trans*-Golgi network as an integral membrane protein. J. Virol. **77:**10630–10637.
61. **Watanabe, T., S. Watanabe, H. Ito, H. Kida, and Y. Kawaoka.** 2001. Influenza A virus can undergo multiple cycles of replication without M2 ion channel activity. J. Virol. **75:**5656–5662.
62. **Watanabe, T., S. Watanabe, T. Noda, Y. Fujii, and Y. Kawaoka.** 2003. Exploitation of nucleic acid packaging signals to generate a novel influenza virus-based vector stably expressing two foreign genes. J. Virol. **77:**10575–10583.
63. **Yewdell, J. W., E. Frank, and W. Gerhard.** 1981. Expression of influenza A virus internal antigens on the surface of infected P815 cells. J. Immunol. **126:**1814–1819.
64. **Zebedee, S. L., and R. A. Lamb.** 1989. Growth restriction of influenza A virus by M2 protein antibody is genetically linked to the M1 protein. Proc. Natl. Acad. Sci. USA **86:**1061–1065.
65. **Zebedee, S. L., and R. A. Lamb.** 1988. Influenza A virus M2 protein: monoclonal antibody restriction of virus growth and detection of M2 in virions. J. Virol. **62:**2762–2772.
66. **Zebedee, S. L., and R. A. Lamb.** 1989. Nucleotide sequences of influenza A virus RNA segment 7: a comparison of five isolates. Nucleic Acids Res. **17:**2870.
67. **Zebedee, S. L., C. D. Richardson, and R. A. Lamb.** 1985. Characterization of the influenza virus M2 integral membrane protein and expression at the infected-cell surface from cloned cDNA. J. Virol. **56:**502–511.
68. **Zhang, J., G. P. Leser, A. Pekosz, and R. A. Lamb.** 2000. The cytoplasmic tails of the influenza virus spike glycoproteins are required for normal genome packaging. Virology **269:**325–334.
69. **Zhirnov, O. P.** 1992. Isolation of matrix protein M1 from influenza viruses by acid-dependent extraction with nonionic detergent. Virology **186:**324–330.
70. **Zhirnov, O. P.** 1990. Solubilization of matrix protein M1/M from virions occurs at different pH for orthomyxo- and paramyxoviruses. Virology **176:** 274–279.